Impact of ring torsion dynamics on intrachain charge transport in conjugated polymers

Magnus Hultell* and Sven Stafström†
Department of Physics, Chemistry and Biology, Linköping University, S-58183 Linköping, Sweden
(Received 25 July 2008; revised manuscript received 4 December 2008; published 9 January 2009)

Based on an approach including both the time-dependent Schrödinger equation and an effective Newton's equation for the ionic motion, we study the impact of ring torsion dynamics on the intrachain charge transport process in conjugated polymers. As model systems we have used single chains of poly(*para*-phenylene-vinylene). Without any external electric field, the dynamics of the phenyl ring torsion is the dominant property controlling intrachain charge propagation. The charge is coupled to both ring torsions and bond lengths distortions, which results in a significantly more localized polaron state than in a planar chain. In the presence of an electric field, the charge can breach the barriers caused by ring torsions, a process that involves nonadiabatic effects and a temporary delocalization of the polaron state.

DOI: 10.1103/PhysRevB.79.014302 PACS number(s): 31.70.Hq, 33.50.Hv, 42.65.Re, 71.35.−y

I. INTRODUCTION

Organic conjugated polymers have emerged as a highly promising class of material for electronic, photovoltaic, and optoelectronic applications, particularly for displays and light emitting diodes (LEDs). Considerable experimental and theoretical efforts have therefore been devoted to the understanding of the basic properties of these materials. Among the most vividly studied prototypical polymers is poly(*para*-phenylene-vinylene) (PPV). In dense films it nominally exhibits a smooth lamellar morphology which resolves in a microfibrillar construction of crystallites embedded in less ordered grain-boundary regions.[1] Within individual crystallites the lateral packing of the polymers assume a herringbone arrangement with two nonequivalent chains per unit cell.[2–5] This arrangement makes it possible to study the electronic properties in both the isolated and the crystalline states.

Refined x-ray diffraction studies on highly oriented PPV samples reveal a nonplanar thermal-averaged chain conformation with thermally driven large-amplitude phenylene ring torsions.[6] The value of the *average* torsion angle $\langle\theta\rangle$ between the plane of the phenylene ring and that of the vinylene segment, as well as the torsional displacement, θ_l, about $\langle\theta\rangle$, were found to increase with temperature: from $\langle\theta\rangle=8°$ and $\theta_l=9°$ at 293 K to $\langle\theta\rangle=13°$ and $\theta_l=18°$ at 673 K above which the solid-state film decomposes. Similar results obtained from neutron-diffraction studies were reported by Mao *et al.*[7]

The vibrational modes in these systems have been studied both experimentally and theoretically. Measuring all-hydrogen and vinylene-deuterated samples using inelastic-incoherent-neutron-scattering (IINS) methods and correlating the peaks in the IINS spectrum with the vibrational modes obtained from Hartree-Fock calculations using the semiempirical Austin model 1 (AM1) method, Papanek *et al.*[8] showed that almost all of the observed vibrational modes in crystalline PPV with frequencies below $\sim$322.62 cm^{-1} can be attributed to ring librations. In particular, they found that both the phenylene rings and the vinylene segments can be regarded as almost rigid units in this low-frequency regime, and that the vibrational modes involves the rotation about and bending of the C-C bonds connecting the phenylene and the vinylene units. These results imply that ring torsion may occur at the same time scale as electron transport, and thus introduce potential barriers for the propagation of the charge carrier since rotation about the C-C single bonds will serve to reduce the electronic coupling between the phenylene rings and the vinylene segments.

Similar effects where recently studied by Prins *et al.*[9] using a combined approach of experiments and numerical simulations. The intrachain mobility was obtained by pulse-radiolysis time-resolved microwave conductivity (TRMC) measurements as a function of the probing frequency for the oscillating microwave field. In studies using this technique the presence of potential barriers leads to an increase in intrachain mobility with probing dc frequency since the high-frequency mobility in these measurements is probed over smaller distances and dominated by the motion of charge carriers in relatively planar regions between barriers. In addition to experiments, Prins *et al.*[9] also performed charge transport simulations that confirmed the observed dependence of intramolecular mobility on probing frequency, and conclusions regarding the upper limit of intrachain mobilities in PPV could be drawn.

To this body of knowledge we wish to add a detailed account of the intramolecular charge transport processes at the microscopic level with the effect of the torsion dynamics specifically taken into account. We also focus on the possible nonadiabatic contributions to the charge transport. The charge carrier can in our approach perform hopping motion, i.e., dynamically make transitions from one eigenstate to another. As such, this study can be regarded as complementary to the previously mentioned work by Prins *et al.*[9] which relies on a more macroscopic approach in which the details of the electron-phonon coupling and the effect of the electric-field strength have been left out.

We have previously studied the impact of static ring torsion on intramolecular charge transport in PPV (Ref. 10) and from those studies obtained conditions for potential-energy barrier crossings due to ring torsion. However, according to the experiments and semiempirical calculations performed by Papanek *et al.*,[8] changes in ring torsion actually occur on the same time scale as charge transport. We have therefore modified our approach in Ref. 10 so as to be able to account

also for the impact of out-of-plane ring torsion modes on the transport of charge along single molecules of PPV. The details of this methodology is given in Sec. II and the results from numerical simulations are presented in Sec. III followed by a summary and conclusions in Sec. IV.

II. METHODOLOGY

In our approach, suitable for conjugated hydrocarbon polymer chains, we obtain the time dependence of the electronic degrees of freedom from the solutions to the time-dependent Schrödinger equation,

$$i\hbar|\dot{\Psi}(t)\rangle = \hat{H}_{\rm el}|\Psi(t)\rangle. \tag{1}$$

Simultaneously to solving Eq. (1) we determine the ionic motion in the evolving charge-density distribution by solving the lattice equation of motion within the potential field of the electrons and the ions,

$$M_i\ddot{\mathbf{r}}_i(t) = -\nabla_{\mathbf{r}_i(t)}\langle\Psi(t)|\hat{H}(t)|\Psi(t)\rangle. \tag{2}$$

Here, $\hat{H}$ ($\hat{H}_{\rm el}$) is the molecular (electronic) Hamiltonian, and $\mathbf{r}_i$ and M_i are the position and mass of the ith atom, respectively. This approach has previously been applied to the case of static phenylene ring torsions in PPV.[10] We will therefore not go into all the details of the methodology but rather limit our discussion to a brief presentation in Sec. II A of the final forms of $\hat{H}$ and Eqs. (1) and (2). In Sec. II B we then present a unique approach of how to incorporate out-of-plane phenylene ring torsion modes in this methodology.

A. Electron-lattice dynamics

For the Hamiltonian, $\hat{H}$, we use a tight-binding model developed from the Su-Schrieffer-Heeger (SSH) model[11] for the polymer chain and assume σ-π separability. In the SSH model the lattice is treated classically, i.e., the operators of the lattice displacements are replaced with their expectation values. The contribution from the π electrons to the Hamiltonian [including the contribution from an externally applied electric field, $\hat{H}_E(t)$, discussed below] can then be written in the form

$$\hat{H}_{\rm el}(t) = -\sum_{\langle nm\rangle}\beta_{nm}(t)[\hat{c}_n^\dagger\hat{c}_m + \hat{c}_m^\dagger\hat{c}_n] + \hat{H}_E(t), \tag{3}$$

where $\langle nm\rangle$ denotes summation over covalently bonded atoms, β_{nm} denotes the resonance integral between the $2p_z$ orbitals on sites n and m, and $\hat{c}_n^\dagger$ ($\hat{c}_n$) denotes the operator for creating (annihilating) an electron on site n. The resonance integrals are treated in the Mulliken approximation[12] with the analytical functions for the overlap integrals taken from Ref. 13. Expanding these integral expressions to first order around the undimerized state, we derive the following equation for the dependence of β_{nm} on the bond-length distortions $\Delta r_{nm}(t)$, and the torsion angle θ_{nm} between the $2p_z$ orbitals on sites n and m along the bond axis:

$$\beta_{nm}(t) = \cos[\theta_{nm}(t)][\beta_0 - \alpha\Delta r_{nm}(t)]. \tag{4}$$

The second factor in this expression is exactly identical to the SSH expression,[11] where β_0 is the reference resonance integral and α is the electron-phonon coupling constant. By deriving this expression from the Mulliken approximation, it follows that the values of β_0 and α are dependent on each other and can be obtained from the two parametrized functions $\beta_0 = A[15+15a\zeta+6(a\zeta)^2+(a\zeta)^3]$ and $\alpha = Aa\zeta^2[3+3a\zeta+(a\zeta)^2]$, where $A = k(e^{-a\zeta}/15)$, a is the undimerized bond-length distance, and $\zeta = 3.07$ Å^{-1}. In the case of PPV, for which $k = 11.04$ eV and $a = 1.4085$ Å,[10] the numerical values of β_0 and α are 2.66 eV and 4.49 eV/Å, respectively. Furthermore, for the systems considered in this work, $\theta_{nm} \neq 0°$ only at those bonds which interconnect the phenylene rings with neighboring vinylene segments. We will henceforth in Sec. III use the short hand notation θ_j, β_j, and Δr_j, respectively, for all θ_{nm}, β_{nm}, and Δr_{nm} associated with C-C phenylene-vinylene bonds indexed by j.

The lattice part of the Hamiltonian is described in the harmonic approximation as[14]

$$H_{\rm latt}(t) = \frac{K_1}{2}\sum_{\langle nm\rangle}[r_{nm}(t)-a]^2 + \frac{K_2}{2}\sum_{\langle nml\rangle}[\vartheta_{nml}(t)-\vartheta_0]^2 + K_3\sum_{\langle nmlk\rangle}\{1-\cos[\theta_{nmlk}(t)-\theta_0]\} + \frac{1}{2}\sum_{n=1}^{N}M_n\dot{\mathbf{r}}_n^2, \tag{5}$$

where the summations run over unique bonds, bond angles, and torsional angles, and K_1, K_2, and K_3 are the force constants associated with deviations in bond lengths $\Delta r_{nm}(t) = r_{nm}(t)-a$, bond angles $\Delta\vartheta_{nml}(t) = \vartheta_{nml}(t)-\vartheta_0$, and torsion angles $\Delta\theta_{nmlk}(t) = \theta_{nmlk}(t)-\theta_0$ from the undimerized planar structure, i.e., $\{a, \vartheta_0, \theta_0\}$, respectively. With PPV as our model system the values of K_2 and K_3 are chosen so as to support out-of-plane ring torsion dynamics while keeping the structural integrity of the molecule, as will be further discussed in Sec. II B below. K_1 is set to 37.0 eV/Å^2.[10] The last term in Eq. (5) denotes the kinetic-energy contribution. Note that the contribution from the torsion angles has been modified with respect to that specified in Ref. 10 so as to account for the possibility of large torsional displacements with respect to θ_0. Furthermore, to prevent chains from an unphysical contraction, we impose the constraint of keeping the sum of the bond lengths constant, i.e., $\Sigma_{\langle nm\rangle}(r_{nm}-a)=0$, by means of the method of Lagrangian multipliers.[15]

The model also takes into consideration the contribution to the Hamiltonian from an externally applied electric field, $\mathbf{E}(t)$, (in the Coulomb gauge) such that

$$\hat{H}_E(t) = -e\sum_n \mathbf{r}_n\mathbf{E}(t)[\hat{c}_n^\dagger\hat{c}_n - 1], \tag{6}$$

with e being the absolute value of the electron charge. If not otherwise specified, $\mathbf{E}(t)$ is directed along the long molecular axis with a smooth turn on between t_s and t_f:

$$E(t) = \begin{cases} 0, & t < t_s, \\ \frac{1}{2}E_0\left[1-\cos\left(\pi\frac{t-t_s}{t_f-t_s}\right)\right], & t_s < t < t_f, \\ E_0, & t > t_f. \end{cases} \tag{7}$$

Having defined the constituent parts of the Hamiltonian $\hat{H}=\hat{H}_{\mathrm{el}}+\hat{H}_{\mathrm{latt}}$, it follows that Eqs. (1) and (2) are coupled via the one-electron density-matrix elements, $\rho_{nm}(t)$, and therefore must be solved simultaneously. There are several approximation levels that can be used to describe electron-lattice dynamics.[16] In the simplest form, the adiabatic approximation, the potential energy, and the ionic forces are derived within the Born-Oppenheimer approximation based on the solution to the time-independent Schrödinger equation. In our case this approach is not valid since, as discussed above, we would like to include electron transfer or hopping events in our model. Nonadiabatic dynamics can be studied either within the mean-field approximation[17,18] or with correlation effects taken into account. In our case, since we are interested in relatively large systems studied over several femtoseconds, we are effectively restricted to the former approximation level. This approach is however the standard approach in studies of electron transport,[18] in which the energy exchange between the electronic system and the lattice is not the dominating process. The mean-field approach is, however, less good in capturing the details of processes such as Joule heating.[16]

Within the mean-field approximation we make the ansatz that the electrons influence the ions via the time-dependent electron density $\rho_{nm}(t)=\Sigma_{\nu=1}^{N}C_{n\nu}^{*}(t)f_{\nu}C_{m\nu}(t)$, where $f_{\nu}\in[0,1,2]$ is the time-independent occupation number of the νth time-dependent molecular orbital $|\psi_{\nu}(t)\rangle$, and $C_{n\nu}(t)$ are the time-dependent expansion coefficients of a linear combination of atomic orbitals, $|\psi_{\nu}(t)\rangle=\Sigma_{n=1}^{N}C_{n\nu}(t)|\phi_{n}\rangle$. Using the generalized Hellmann-Feynman theorem for the ionic forces,[17] Eq. (2) then resolves into

$$M_{n'}\ddot{\mathbf{r}}_{n'}(t)=-\sum_{\nu=1}^{N}\sum_{n,m=1}f_{\nu}C_{n\nu}^{*}(t)\langle\phi_{n}|\nabla_{\mathbf{r}_{n'}}\hat{H}(t)|\phi_{m}\rangle C_{m\nu}(t), \quad (8)$$

where the expansion coefficients $C_{n\nu}(t)$ are obtained from the following equation derived from Eq. (1):

$$i\hbar\dot{C}_{n\nu}(t)=-e\mathbf{r}_{n}\mathbf{E}_{0}(t)C_{n\nu}(t)-\sum_{m\in\langle nm\rangle}\beta_{nm}(t)C_{m\nu}(t). \quad (9)$$

The coupled differential Eqs. (8) and (9) are solved numerically using a Runge-Kutta method of order 8 with step-size control,[19] which in practice means a time step of about 10 as. Furthermore, we use a "global time step" of 1 fs and take as the starting wave function the solution to the time-independent Schrödinger equation of the atomic configuration at $t=0$ fs.

Finally, in order to study also the nonadiabaticity of the charge transport process, we expand the electronic states $|\psi_{\nu}(t)\rangle$ in a basis of instantaneous eigenstates as follows:

$$|\psi_{\nu}(t)\rangle=\sum_{\mu=1}^{N}\alpha_{\nu\mu}(t)|\varphi_{\mu}\rangle, \quad (10)$$

where $\alpha_{\nu\mu}(t)=\langle\varphi_{\mu}|\psi_{\nu}(t)\rangle$ and $|\varphi_{\mu}\rangle$ are the solutions to the time-independent Schrödinger equation at that instant. The time-dependent occupation number of the instantaneous eigenstates ν can then be obtained as[18]

$$n_{\nu}(t)=\sum_{\mu=1}^{N}f_{\mu}|\alpha_{\nu\mu}(t)|^{2}. \quad (11)$$

B. Torsional force constant

In order to obtain reference values for the frequencies and magnitudes of out-of-plane phenylene ring torsion in PPV, we employed the TINKER software package[20] and performed a set of molecular-dynamics (MD) simulations at room temperature on small PPV oligomers such as *trans*-stilben. For these simulations we used an MM3 force field and a modified Pariser-Parr-Pople (PPP) method for the self-consistent field (SCF) molecular-orbital calculations for the π system. In particular, we find that the time period for the torsion of the phenylene rings with respect to the vinylene segment in *trans*-stilben is roughly 1.4 ps. With this as a reference, we determine the value of K_3 in Eq. (5), which regulates the time period for phenylene ring torsion in our model, to be $K_3\simeq 0.1$ eV.[21] As previously discussed, there are a number of different frequencies reported in the literature for the torsional modes in PPV.[8] In the simulations discussed in Sec. III, we have therefore considered also other values of K_3.

Another feature of phenylene ring torsion dynamics, as pointed out by Papanek *et al.*,[8] is that the motion of the rings is decoherent. This feature can be introduced into our system by initiating the system in a coherent state, e.g., with $\theta_j(0)\neq 0°$ and $\theta_0=0°$, and wait for the system to reach the decoherent state. This process is, however, extremely time consuming and thus not suitable even for very small systems. Instead, we chose to initiate the system with all phenylene ring torsions fixed to the same value $[\{\theta_j(0)\}=0°$, 10°, and 20°] and let the torsion dynamics for each individual phenylene ring start randomly during a certain period of time (typically 900 fs). By means of this deterministic initiation procedure, the time evolution of phenylene ring torsion in the system, and thus also the resonance integral strength [see Eq. (4)], will be uniquely defined. It should be emphasized that, however, the charge transport processes observed in systems with different random sequences in the order in which the torsions start do not differ qualitatively from each other, wherefore the results presented and discussed below represent general features of this type of system.

For future references it should also be pointed out that the kinetic energy in our system is lower than in real PPV oligomers due to the restriction of keeping all torsion angles other than $\{\theta_j\}$ at 0° (or 180°). The fact that not all degrees of freedom are activated means that we cannot calculate the temperature directly from the average kinetic energy. Instead, we have made comparison with molecular-dynamics simulations on PPV oligomers. These simulations show a standard deviation in the distribution of $\{\theta_j\}$ of 24° at room temperature,[22] which is in good agreement with the large-amplitude initial value of $\{\theta_j\}|_{t=0}=20°$ used in this work. The smaller amplitude value of $\{\theta_j\}|_{t=0}=10°$ also studied here corresponds consequently to low temperatures.

III. RESULTS

The first simulation results that are presented here concern ring torsion dynamics along the PPV chain for different tor-

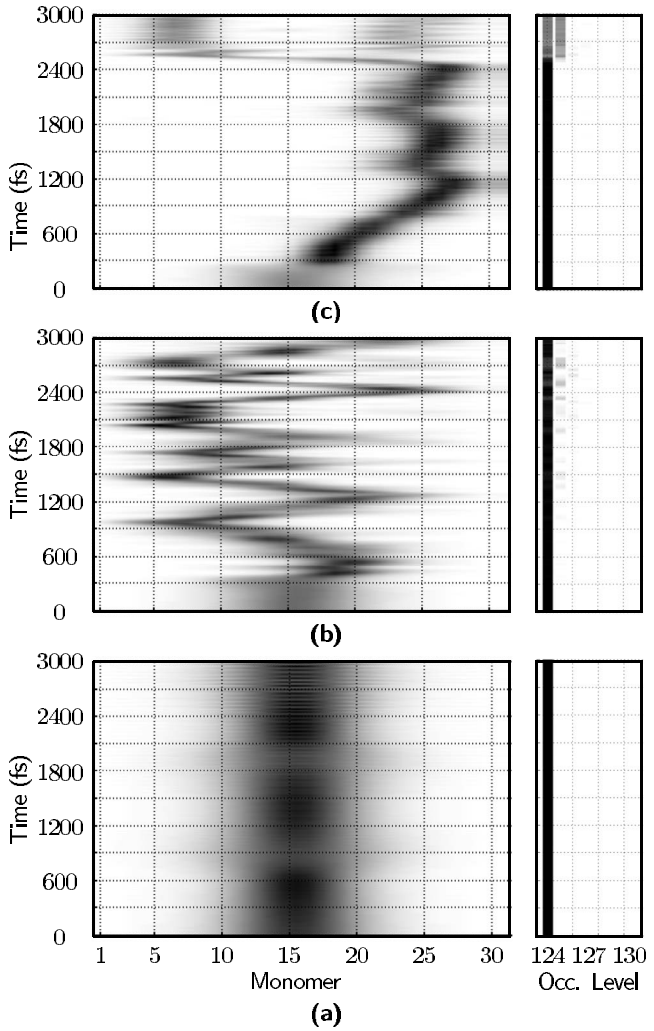

FIG. 1. The left panels of (a)–(c) show the time evolution of the density of charge per monomer in PPV oligomers with 31 phenylene rings and identical onset procedures for ring torsion dynamics but with different initial torsion angles at $\{\theta_j\}|_{t=0}=0°$, 10°, and 20°, respectively. The right panels of (a)–(c) show the corresponding time evolution of the occupation number of the instantaneous eigenstates.

sion angle amplitudes. The chain is charged with one additional electron but without an external electric field applied (unbiased system). It is well known that an additional charge on a PPV oligomer self localizes and forms a polaron state with the added charge spread over approximately six phenylene-vinylene units.[15] In Figs. 1(a)–1(c) are shown the results for PPV oligomers with 31 rings and initial torsion angles, $\{\theta_j\}|_{t=0}$, at 0°, 10°, and 20°, respectively. The left panels display the time evolution of the net charge density per monomer, i.e., the charge density associated with the polaron, and in the right panels the corresponding dynamics of the occupation number [Eq. (11)] of the instantaneous eigenstates are shown.

In the case of $\{\theta_j\}|_{t=0}=0°$ the polaron is stable and resides at the center of the chain as expected for a finite sized system. The presence of an acoustic phonon bouncing back and forth through the system does, however, introduce a periodic fluctuation in the density of charge. The width of the polaron agrees with that observed in an earlier work.[15]

A dramatic change in the behavior of the system occurs when the torsion dynamics is initiated. In the left panels of Figs. 1(b) and 1(c) for the systems with $\{\theta_j\}|_{t=0}=10°$ and 20°, we no longer observe a polaron resting at the middle of the PPV chain but rather a diffusive propagation of the charge carrier spurred into motion by the presence of ring torsion motion. We also find that the polaron motion is much more restricted in the system with $\{\theta_j\}|_{t=0}=20°$ than for $\{\theta_j\}|_{t=0}=10°$ and that it moves more slowly through the former system due to the greater impact of ring torsion on the reduction in the resonance integral strength, β_j [see Eq. (4)].

Another important observation is that the polaron is considerably more localized when $\theta_j(0)\neq 0°$ compared to the completely planar system. For $\{\theta_j\}|_{t=0}=20°$ the polaron extends over two to three phenylene-vinylene units only. This is a consequence of the increase in total electron-phonon coupling which results from the cosine term in Eq. (4). We also note that the polaron can be destabilized by the motion of the phenylene rings. This is the case at $t\sim 2600$ fs in the system with $\{\theta_j\}|_{t=0}=20°$ and we observe in the left panel of Fig. 1(c) a delocalization of charge to two different regions of the system. From the right panel of Fig. 1(c) it is clear that this is a nonadiabatic event with the simultaneous occupation of two instantaneous eigenstates. Multiple level occupation of this kind is also observed in the occupation spectrum for the system with $\{\theta_j\}|_{t=0}=10°$ but correlates in this case to events when the charge carrier breaches potential-energy barriers introduced through the dynamics of ring torsion.

To obtain a more detailed picture of the dynamics that governs diffusive charge transport processes, we reproduce in the left panel of Fig. 2 the time evolution of the density of charge per monomer displayed already in the left panel of Fig. 1(c) for a PPV oligomer with $\{\theta_j\}|_{t=0}=20°$ (corresponding to room temperature) and in the right panel the corresponding dynamics of the resonance integrals, β_j, across each interconnecting bond between a phenylene ring and a vinylene group in that system. Also displayed in the right panel of Fig. 2 is the superimposed trace of the center of the local density of charge. Keeping in mind that β_j does not change in time before the onset of ring torsion and that the darker regions in the right panel of Fig. 2 represent weak resonance integrals, it is obvious by following the trace of the polaron that the charge carrier is localized by the dynamics of the lattice to regions with consistently large values of the resonance integrals. According to Eq. (4) the modulation of β_j is governed by the dynamics of both θ_j and the variations in the interatomic distance across the associated bond. However, when comparing the time evolution of these three quantities, it is found that the modulation of β_j due to bond-length variations Δr_j is less pronounced than that for θ_j and of a much higher frequency than that observed in the right panel of Fig. 2. The correlation between the dynamics of θ_j and β_j is, however, very strong. We therefore conclude that the intrachain diffusive charge transport process in PPV oligomers is controlled by the dynamics of ring torsion. Note though that the bond-length vibrations are responsible for high-frequency shifts in the position of the center of the polaron between two neighboring monomers, which are also visible in Fig. 1.

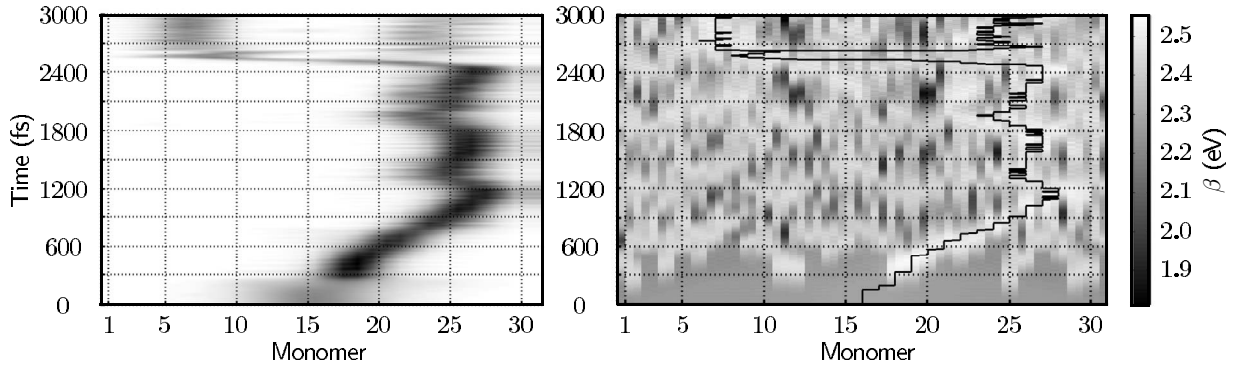

FIG. 2. The left panel shows the time evolution of the density of charge per monomer in a PPV chain with 31 phenylene rings and initial torsion angles at $\{\theta_j\}|_{t=0}=20°$. The net charge density is depicted in grayscale. The right panel displays the resonance integral strength, β, across each bond between a phenylene ring and a vinylene group in this system. The grayscale to the right shows the value of β in electron volts. Note that the dark regions represent low values of β, which act as barriers for charge transport. The solid line in the right panel indicates the position of the center of the local density of charge in the left panel.

As discussed above, in the model we are using, the value of K_3 (and therefore also the torsional frequency) has been determined on the basis of MD simulations. In the literature there are reports of different frequencies[8,9] of the normal modes associated with the torsional degrees of freedom. In order to incorporate a wider range of such possible frequencies in our study, we have performed simulations similar to those shown in Figs. 1 and 2 but with different values of K_3 in the range from 0.01 to 1.0 eV. The results from these simulations show that it is only the time scale of the system dynamics that changes with the value of K_3: the lower the torsional frequency is the longer time it takes for the charge to traverse the system, but the principal dynamical behavior remains the same.

Due to the close correspondence between β_j and θ_j, the right panel of Fig. 2 also provides a fair representation of the ring torsion dynamics in the system. We note that while some ring torsion angles are suppressed others are enhanced such that the maximum torsion angles observed during the dynamics of the system actually reaches as high as 35° (given an initial torsion angle $\{\theta_j\}|_{t=0}=20°$), which, e.g., is the case for θ_{40} and θ_{41} of the 20th phenylene ring at $t\simeq 2.2$ ps. A similar behavior is also observed in the molecular-dynamics simulations we have performed.[22]

Following the polaronic trace superimposed on the dynamics of β_j in the right panel of Fig. 2, we have identified three mechanisms that influence the diffusive motion of polaronic charge carriers in this type of systems. The first is the evolution of regions with low values of β_j that act as potential-energy barriers for polaron propagation.[23] The second is the evolution of regions along the chain where the resonance integrals are consistently strong and toward which the polaron is attracted. The interplay between these two mechanisms is such that the polaron will localize to the region of the chain with the highest values of β_j provided that the charge carrier is able to breach the intersecting potential-energy barriers that arise due to ring torsion. A third mechanism for diffusive polaron motion also comes into play in the event of a sudden increase in one or several resonance integrals within the region where the polaron resides. This will push the polaron away from its current location. Such an event can actually serve to destabilize the polaron and force the density of charge to localize to two separate regions of the chain as observed, e.g., in the left panels of Figs. 1(c) and 2 toward the end of the simulation.

Having so far treated only diffusive propagation of polarons in systems subjected to dynamic ring torsion, we shall now consider also polaronic motion under the influence of an external electric field (biased system). For this purpose we repeat the previously detailed simulations associated with the results presented in Fig. 1 but with the external electric field supplied in accordance with Eq. (7). It is found that, while the onset of the electric field has a significant impact on the dynamics of the charge carrier, it is of little importance for the dynamics of ring torsion throughout the system. This explains why the time evolution of the resonance integral strength depicted in the right panels of Fig. 2, and of Figs. 3(a) and 3(b) are very similar.

The left panels of Fig. 3 show the time evolution of the density of charge per monomer for two PPV oligomers with identical initial-state configuration and onset conditions to the system in the left panel of Fig. 2. The center panels in Fig. 3 show the time evolution of the occupation number of the instantaneous eigenstates associated with the two systems. In the right panels are displayed the time evolution of β_j.

The external electric field is switched on at $t_s=1400$ fs and raised from $E(t_s)=0$ V/cm to $E(t_f)=5.0\times 10^4$ V/cm during $t_f-t_s=25$ [Fig. 3(a)] and 200 fs [Fig. 3(b)], respectively, which are time periods that are highlighted in the left panels of Figs. 3(a) and 3(b) using solid horizontal lines to indicate t_s and t_f. After this switch-on period the electric-field strength is kept at $E(t_f)=5.0\times 10^4$ V/cm, a field strength which represents typical values in organic electronic devices.[24] With reference to the dynamics of β_j displayed in the right panels of Figs. 3(a) and 3(b), this means that the field is introduced at a point in time when the charge is localized to a narrow region around the 26th monomer. Under these circumstances the actual breaching of the barrier by the localized charge depends on the relation between the height of the barrier and the strength of the electric field, and consequently also on the duration of the onset of the electric field, t_f-t_s [see Eq. (7)].

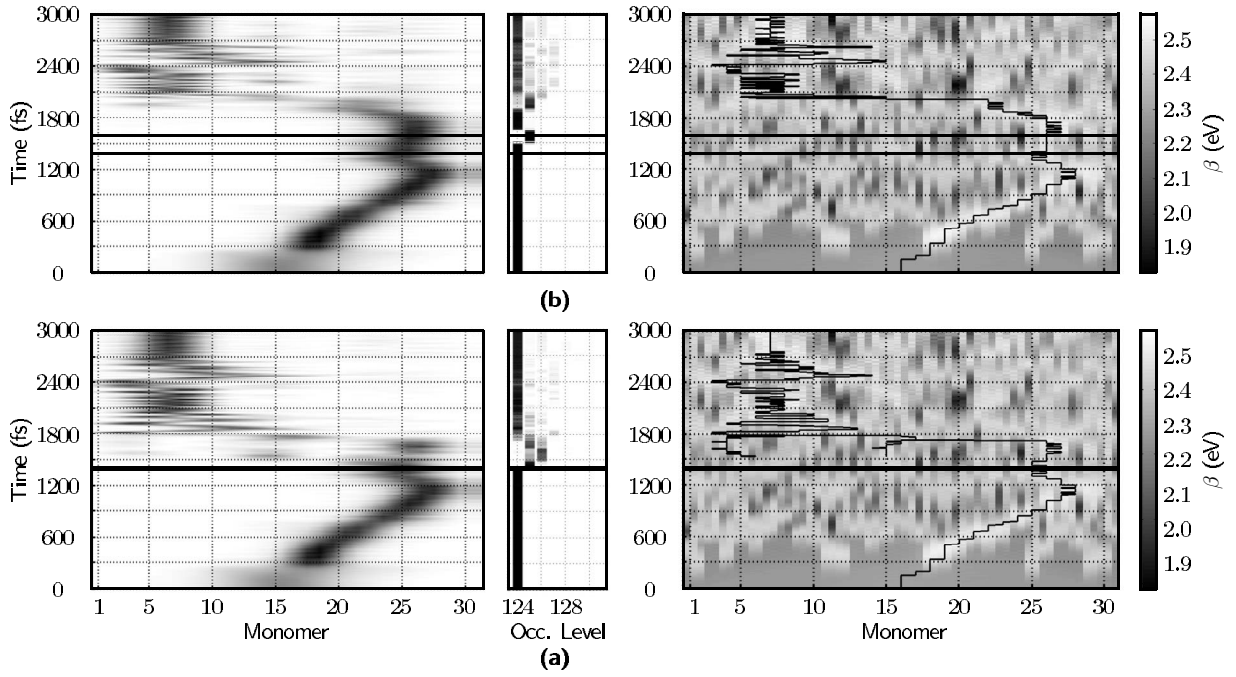

FIG. 3. The left panels of (a) and (b) show the time evolution of the density of charge per monomer in two PPV chains with 31 phenylene rings and initial torsion angles at $\{\theta_j\}|_{t=0}=20°$ but with an external electric field ($E_0=5.0\times10^4$ V/cm^2) switched on smoothly at $t_s=1400$ fs over a time period of (a) 25 and (b) 200 fs, respectively. The solid horizontal lines indicate t_s and t_f. Note that in (a) these two times appear as one thicker line due to the short switch-on time. In the center panels are shown the corresponding time evolutions of the occupation number per molecular level. The LUMO of the neutral system is molecular level 124, followed by LUMO+1 (125), LUMO+2 (126), etc. The right panels show the time evolutions of the resonance integral strength across each bond between a phenylene ring and a vinylene group. The grayscale to the right shows the value of β in electron volt. Note that the dark regions represent low values of β, which act as barriers for charge transport. The solid lines in the right panels indicate the positions of the center of the local density of charge in the left panels.

Most of the discussion related to the results displayed in Fig. 3 relate to the simulation performed with the longer switch-on time (200 fs) of the electric field. In this case there are no nonadiabatic effects caused by the switch-on process itself and the charge transport dynamics occurs at a time $t>t_f$. In the simulations with $t_f-t_s=25$ fs, the switch-on itself induces nonadiabatic effects as can be seen from Fig. 3(a). These effects themselves lead to transport of the charge along the chain and the dynamics is in this case largely dependent on extrinsic effect, i.e., the switch-on time. This result of such a nonadiabatic switch-on procedure is worth noting but will not be discussed further in this work.

With reference to the dynamics displayed in Fig. 3(b) in between $t=1400$ and 1800 fs, the situation may arise when the charge carrier approaches a region where the torsion of phenylene rings is so strong and the corresponding potential-energy barriers consequently so high that not even the assistance of the electric field will enable the charge carrier to breach the barrier at a certain point in time. Eventually, however, the barrier height is reduced by the torsion dynamics of the rings and the charge carrier will be able to continue to propagate through the system. For the simulation displayed in Fig. 3(b) this occurs at $t=1900$ fs. However, the propagation is not an adiabatic polaron drift process. Instead we observe a temporary destabilization of the polaron and a corresponding change in the occupation from level 124 [which is the lowest unoccupied molecular orbital (LUMO) level of the neutral system] to level 125. Thus, there is a clear signature of a nonadiabatic charge-transfer process in this case. The destabilization of the polaron is due to the fact that the acceptor level (level 125) initially is quite delocalized. We also notice that this state, when it becomes occupied, stabilizes due to the electron-phonon coupling, and after around 200 fs (at $t=2100$ fs) it crosses the donor level (level 124) and becomes the lowest occupied molecular orbital.

The fact that the charge carrier actually transverses the PPV chain despite the presence of barriers caused by ring torsions shows that the hopping contribution to the charge transport is very important. Intrachain charge transport in the presence of an external electric field is obviously not dramatically limited by the disorder caused by the dynamics of the ring torsions.

Correlating the dynamics of the time-dependent occupation number displayed in the center panels of Figs. 3(a) and 3(b) with the dynamics of the charge density (left panels) and the resonance integrals (right panels), we find that the actual transition across the barrier involves a situation where the charge density and the occupation number split between multiple regions and multiple instantaneous eigenstates, respectively. Such nonadiabatic transitions are likely to increase in numbers with increased amplitudes of ring torsion since the number of barriers with a height that requires the assistance of the electric field for the charge carrier to be able to traverse the system then also increases. In other words, mul-

tiple occupancy of instantaneous eigenstates is more of a commonality in systems with higher magnitudes of ring torsion angles than in those systems where θ_j is lower, provided that the field is sufficiently strong for the charge carrier to actually breach the potential-energy barrier induced by the dynamics of ring torsion.

IV. SUMMARY AND CONCLUSIONS

We have studied charge-carrier propagation along PPV chains with the dynamics of out-of-plane ring torsion included. The phonons associated with this type of lattice dynamics are decoherent and of such high frequencies that the modulation of the resonance integrals at the C-C phenylene-vinylene bonds due to dynamic ring torsion only impose temporary restrictions of localization on propagating charge carriers. Further insight into the transport processes at hand is gained from simulations on both unbiased and biased systems. In particular, we find that charge carriers in the unbiased systems move as a consequence of the continuous changes made to the potential-energy surface by the dynamics of ring torsion. Also, we find that nonadiabatic occupation of multiple levels arise when charge carriers are either destabilized by the torsion of rings within the region where it resides or when the charge carrier breaches a potential barrier. Our results also provide a detailed description of the charge transport process in the biased systems. We show that the introduction of ring torsions can lead to nonadiabatic transport. The transport process involves a transition from the localized polaron level to a delocalized level, followed by stabilization of this delocalized level into another polaronic state. Thus, intrachain charge transport involves both nonadiabatic effects and the dynamics of the polaron state.

ACKNOWLEDGMENTS

Financial support from the Center of Organic Electronics (COE), Swedish Foundation of Strategic Research, is gratefully acknowledged.

*mahul@ifm.liu.se
†sst@ifm.liu.se

[1] M. A. Masse, D. C. Martin, E. L. Thomas, F. E. Karasz, and J. H. Petermann, J. Mater. Sci. **25**, 311 (1990).
[2] D. Gagnon, F. E. Karasz, E. L. Thomas, and R. W. Lenz, Synth. Met. **20**, 85 (1987).
[3] D. D. C. Bradley, R. H. Friend, T. Hartmann, E. A. Marseglia, M. M. Sokolowski, and P. D. Townsend, Synth. Met. **17**, 473 (1987).
[4] T. Granier, E. L. Thomas, D. R. Gagnon, R. W. Lenz, and F. E. Karasz, J. Polym. Sci., Polym. Phys. Ed. **24**, 2793 (1986).
[5] T. Granier, E. L. Thomas, and F. E. Karasz, J. Polym. Sci., Part B: Polym. Phys. **27**, 469 (1989).
[6] D. Chen, M. J. Winokur, M. A. Masse, and F. E. Karasz, Polymer **33**, 3116 (1992).
[7] G. Mao, J. E. Fischer, F. E. Karasz, and M. J. Winokur, J. Chem. Phys. **98**, 712 (1993).
[8] P. Papanek, J. E. Fischer, J. L. Sauvajol, A. J. Dianoux, G. Mao, M. J. Winokur, and F. E. Karasz, Phys. Rev. B **50**, 15668 (1994).
[9] P. Prins, F. C. Grozema, and L. D. A. Siebbeles, J. Phys. Chem. B **110**, 14659 (2006).
[10] M. Hultell and S. Stafström, Phys. Rev. B **75**, 104304 (2007).
[11] W. P. Su, J. R. Schrieffer, and A. J. Heeger, Phys. Rev. Lett. **42**, 1698 (1979).
[12] R. S. Mulliken, J. Chem. Phys. **46**, 675 (1949).
[13] R. S. Mulliken, A. A. Reike, D. Orloff, and H. Orloff, J. Chem. Phys. **17**, 1248 (1949).
[14] S. N. Ha, A. Giammona, and M. Field, Carbohydr. Res. **180**, 207 (1988).
[15] Å. Johansson and S. Stafström, Phys. Rev. B **68**, 035206 (2003).
[16] A. P. Horsfield, D. R. Bowler, A. J. Fisher, T. N. Todorov, and C. G. Sánchez, J. Phys.: Condens. Matter **16**, 8251 (2004).
[17] R. E. Allen, Phys. Rev. B **50**, 18629 (1994).
[18] H. W. Streitwolf, Phys. Rev. B **58**, 14356 (1998).
[19] R. W. Brankin and I. Gladwell, RKSUITE_90: Software for ODE IVPs (www.netlib.org).
[20] J. W. Ponder, TINKER 4.2: Software tools for Molecular Mechanics (http://dasher.wustl.edu/tinker/).
[21] In these simulations we used the value $K_2=20$ eV/rad^2, which is lower than what has previously been used for PPV (Ref. 10) but required in order to keep the structural integrity of the chain during simulation. Note that, even with $K_2=20$ eV/rad^2 we are still able to obtain a good reproduction of the neutral ground-state configuration as well as to reproduce the charge-carrier dynamics observed in Ref. 10.
[22] M. Linares, M. Hultell, and S. Stafström (unpublished).
[23] A detailed account of the dependence of intrachain mobility on the nature of the potential barriers caused by ring torsion in PPV can be found in Ref. 10.
[24] V. Coropceanu, J. Cornil, D. A. da Silva Filho, Y. Olivier, R. Silbey, and J.-L. Brédas, Chem. Rev. (Washington, D.C.) **107**, 926 (2007).